

Prediction of Nonlinear Behavior of Steel Coupling Beams under Seismic Loads Based on Experimental Results

E. Norouzzadeh Tochaei, M. Khanmohammadi & M. Arabpanahan
College of Engineering, School of Civil Engineering, University of Tehran, Tehran, Iran



SUMMARY:

Coupled shear wall with steel coupling beam is one of the hybrid structures that can provide an efficient structural system to resist horizontal force due to earthquake. On the other hand, recently much effort has been devoted to the development of dependable analytical tools for modeling component deterioration and prediction of global collapse of structural systems under seismic loading. Lack of data to model deterioration properties of structural components does not enable us to predict collapse in a reliable manner. This paper focuses on the proposal of relationships that associate deterioration model parameters with detailing, geometric and material properties that control deterioration of steel coupling beam. For calibration and validation of these models existing experimental results will be gathered from technical literatures. Based on information deduced from tests relationships for modelling of effective stiffness, yield strength, capping strength, cyclic deterioration, pre-capping and post-capping plastic rotation for steel coupling beams are proposed.

Keywords: Coupled shear wall, Steel coupling beam, Component deterioration, Moment-rotation relationships

1. INTRODUCTION

In recent years, the use of hybrid system that combines the advantage of steel and reinforced concrete structures has gained popularity. One of these hybrid structures consist of reinforced concrete shear wall with steel coupling beams, which in this paper is named as “coupled shear wall”. Nowadays, coupled shear wall systems have been employed as the lateral force resisting systems for building in the 40-70 story range.

In the past decade, various experimental programmes were under taken to address the lack of information on the steel coupling beam behaviour. Shahrooz et al. (1993) demonstrated that the steel coupling beam exhibit very stable hysteresis curves with little loss of strength. The results of experimental programs have shown that it is possible to achieve excellent ductility and energy absorption characteristics by carefully designing and detailing the steel coupling beams and the reinforced concrete embedment regions (Harries 1995; Harries et al. 1993). Park and Yun (2006a; 2005a,b) had confirmed that the critical shear failure is more reasonable for rehabilitation or retrofitting when the intensity of building damage is taken into consideration by observing the failure modes and hysteretic response of steel coupling beams. A series of experimental tests indicated that the nominally reinforced encasement around steel coupling beams and effect of floor slab may increase the stiffness of coupling beams (Gong and Shahrooz 2001a,b).

Detail of steel coupling beams and embedment region can effect on the behaviour of coupling beams under cyclic loads. Detail of steel coupling beam is shown in Fig. 1.1. Park and Yun (2006b) indicated that by using stud bolts and horizontal ties in embedment region, the behaviour of steel coupling beam can be improved under cyclic loading. The impact of utilizing horizontal ties and face bearing plate on performance of steel coupling beam was investigated by Park and Yun (2006c,d). In an effort to protect the wall piers from local damage around the coupling beams, a system involving a central fuse

has been examined (Fortney et al. 2007a,b; Fortney 2005). The fuse is to act as a repairable or replaceable “weak link” where the inelastic deformations are concentrated while the remaining components of the system are to remain elastic.

In this paper the primary focus is to provide information for the missing aspects of comprehensive modeling of the deterioration characteristics of steel coupling beams based on experimental results that has been gathered from technical literatures. The experimental data is used to calibrate deterioration parameters of the phenomenological deterioration model summarized in the next section, and to develop relationships that associate parameters of this deterioration model with detailing, geometric and material properties that control deterioration in steel coupling beams.

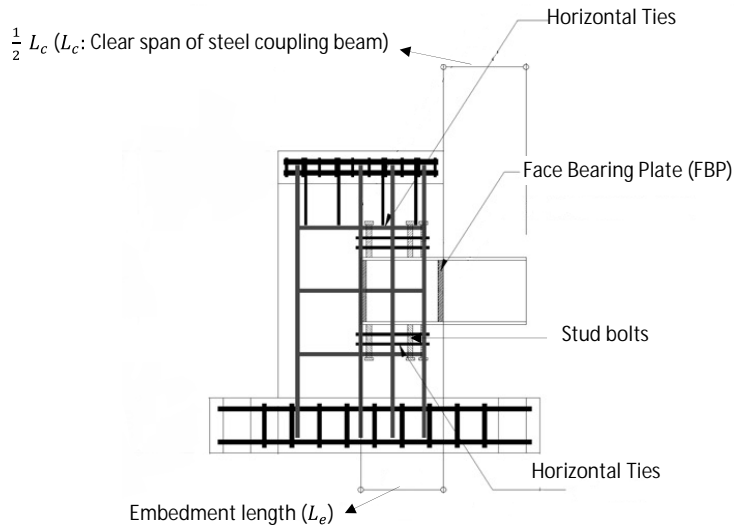


Figure 1.1. Details of steel coupling beam

2. DETERIORATION MODEL

In order to model deterioration characteristics of steel coupling beams, a modified version of the Ibarra-Krawinkler (IK) deterioration model (Lignos et al. 2008) is used in this paper. This model is based on a backbone curve (see Fig. 2.1) that defines a reference boundary for the behavior of a structural component and a set of rules that define the basic characteristics of the hysteretic behavior between the bounds defined by the backbone curve. For a bilinear hysteretic response three modes of deterioration are defined with respect to the backbone curve (see Fig. 2.1). The three modes are: Basic strength, post-capping strength and unloading stiffness deterioration. Ibarra et al. (2005) reported an additional mode of accelerated reloading stiffness deterioration that is typical for peak-oriented and pinched hysteretic behavior. The cyclic deterioration rates are controlled by a rule developed by Rahnama and Krawinkler (1993) that is based on the hysteretic energy dissipated when the component is subjected to cyclic loading. The main assumption is that every component has a reference hysteretic energy dissipation capacity E_t , regardless of the loading history applied to the component. The reference hysteretic energy dissipation capacity is expressed as a multiple of $M_y \cdot \theta_p$, i.e., $E_t = \lambda \cdot M_y \cdot \theta_p$, or, $E_t = \Lambda \cdot M_y$ with $\Lambda = \lambda \cdot \theta_p$ denoting the reference cumulative deformation capacity.

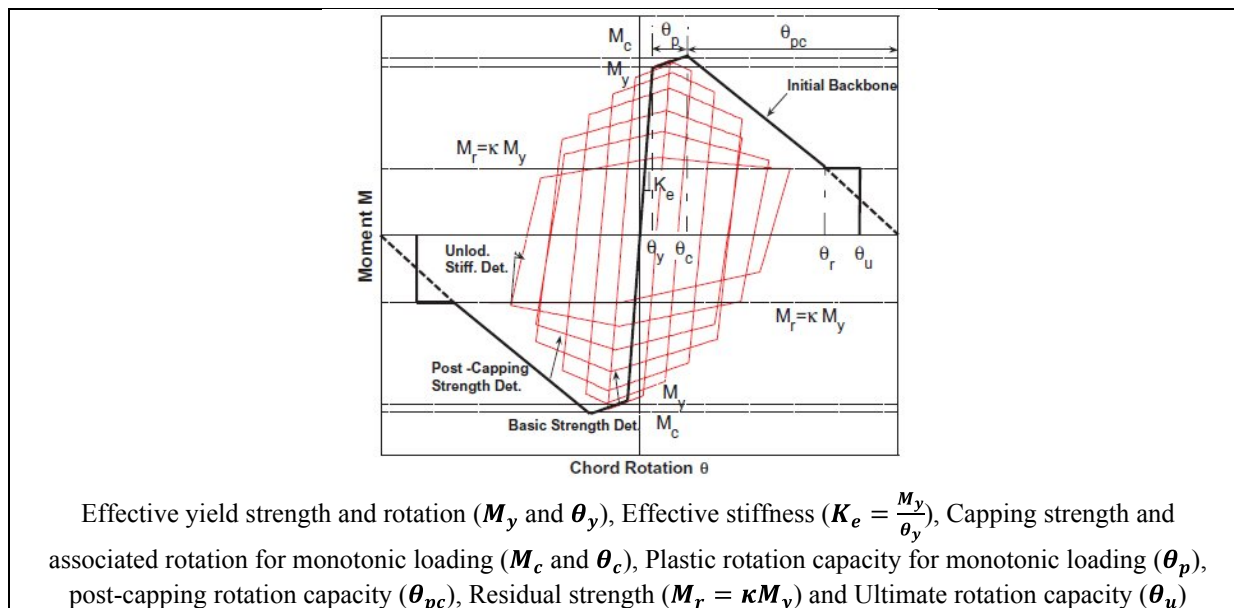


Figure 2.1. Modified Ibarra-Krawinkler (IK) model. Backbone curve, basic modes of cyclic deterioration and associated definitions (Lignos et al. 2009).

3. EXPERIMENTAL DATABASE AND CALIBRATION

3.1. Data Gathering Based on Experimental Tests

In this step, the information of experimental tests on the steel coupling beams are collected from technical literatures (see table 3.1). The database contains data in following categories: geometric properties of components (wall and steel coupling beams), material properties of components, loading history, detailing and reported results (including hysteretic load-displacement response or moment-rotation response).

Cyclic response data of all of experiments were received in paper format. Force-deformation response of these tests had to be manually digitized from research reports.

Table 3.1. Geometric and material properties of components of components (wall and steel coupling beams)

Researcher(s)	Specimen name	$\frac{d}{t_w}$	$\frac{b_t}{t_f}$	$\frac{L_c}{L_e}$	$\frac{L_c}{h}$	$\frac{h}{b_f}$	f_{yw}	f'_c
Park and Yun (2006a; 2005a,b)	SBVRF	46.86	15.91	2.67	2.29	2.00	339	30
	SCF	31.71	15.91	2.00	2.46	1.39	339	30
	FCF	31.71	15.91	4.00	4.92	1.39	339	30
Gong and Shahrooz (2001a,b)	CB1	25.31	6.42	3.76	5.34	1.49	283	14
	CB2	25.31	6.42	3.76	5.34	1.49	283	12
	CB3	25.31	6.42	3.76	5.34	1.49	283	15.8
	CB4	25.31	6.42	3.76	5.34	1.49	283	14.3
	WB1	25.31	6.42	2.37	5.34	1.49	283	57.9
	WB2	25.31	6.42	2.37	5.34	1.49	283	57.7
	WB3	25.31	6.42	2.37	5.34	1.49	283	51.7
Harries (1995), Harries et al. (1993)	S1	61.80	7.11	2.00	3.46	2.57	320	25.9
	S2	61.80	7.11	2.00	3.46	2.57	293	43.1
	S3	55.50	15.88	0.90	1.29	2.75	403	32.9
	S4	55.50	15.88	2.00	3.44	2.75	403	35
Shahrooz et al. (1993)	Wall 1	16.28	8.12	0.62	1.17	2.25	234	35
	Wall 2	16.28	8.12	0.70	1.17	2.25	234	35
	Wall 3	16.28	8.12	1.05	1.17	2.25	234	35

Fortney et al. (2007a,b), Fortney (2005)	SCB	25.43	5.00	1.18	2.57	2.80	245	35.4
	FCB-1	25.43	5.00	1.18	2.57	2.80	250	36.5
	FCB-2	25.43	5.00	1.18	2.57	2.80	244	36.5
Park and Yun (2006b)	HCWS-ST	46.86	15.91	2.67	2.29	2.00	352	30
	HCWS-SB	46.86	15.91	2.67	2.29	2.00	352	30
Park and Yun (2006c,d)	PSF	29.00	11.67	2.00	3.43	1.00	339	30
	PSFF	29.00	11.67	2.00	3.43	1.00	339	30
	PSFFT	29.00	11.67	2.00	3.43	1.00	339	30
Park et al. (2005)	SCB-ST	46.86	15.91	3.21	3.43	2.00	339	34
	SCB-SB	46.86	15.91	3.21	3.43	2.00	339	34
	SCB-SBVRT	46.86	15.91	3.21	3.43	2.00	339	34

In table 3.1 and next sections of this paper:

$\frac{d}{t_w}$: web depth (mm) to web thickness (mm) ratio, $\frac{b_t}{t_f}$: flange width (mm) to flange thickness (mm) ratio, $\frac{L_c}{L_e}$: clear span of beam (mm) to embedment length (mm) ratio (see Fig. 1.1), $\frac{L_c}{h}$: clear span of beam (mm) to beam height (mm) ratio, $\frac{h}{b_f}$: beam height (mm) to flange width (mm) ratio, f_{yw} : yield strength of web (MPa) and f'_c : Concrete Compressive strength (MPa)

3.2. Calibration

In order to calibration of cyclic response data, a modified version of the IK deterioration model is used. For each experiment of the database discussed in section 3.1, parameters of the modified IK model were determined by matching the digitized moment-rotation response to a hysteretic response controlled by the backbone curve (shown in Fig. 2.1) and a cycle deterioration parameter. A combination of engineering mechanics concept and visual observation is employed to select appropriate parameters and pass judgment on satisfactory matching. For this purpose OPENSEES software was used for generating hysteretic response based on deterioration parameters of modified IK model. One example of a satisfactory calibration of the modified IK deterioration model is shown in Fig. 3.1.

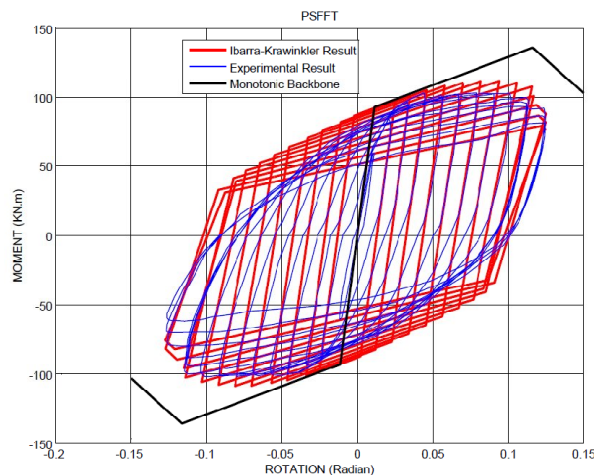


Figure 3.1. Calibration of deterioration model for PSFFT (Park and Yun 2006c,d).

4. RELATIONSHIPS TO MODEL STEEL COUPLING BEAMS

4.1. Multivariate Regression Analysis

After calibration of 28 moment-rotation diagrams for steel coupling beams, the emphasis is on identification of trends of deterioration parameters with respect to important parameters of steel coupling beam.

The dependence of effective yield moment M_y of steel coupling beams on the beam height (h) to flange width (b_f) ratio $\frac{h}{b_f}$ is illustrated in Fig. 4.1. In the same figure a linear regression line is superimposed to illustrate the trend between M_y and $\frac{h}{b_f}$

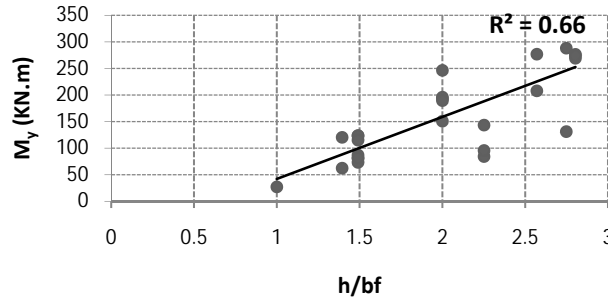


Figure 4.1. Effect of $\frac{h}{b_f}$ on M_y of steel coupling beams

After identifying critical parameters that affect the steel coupling beam deterioration, we are able to propose relationships for modeling of deterioration parameters (backbone curve parameters θ_p , θ_{pc} , K_e , M_y , $\frac{M_c}{M_y}$ cyclic deterioration parameters Λ) of plastic hinge regions in steel coupling beams.

The proposed relationships are empirical, since they are developed with the use of multivariate regression analysis and using the experimental data discussed in Section 3. The trends are not always well defined and the data exhibits large scatter. This affected the regression analysis, and in some cases pure statistics had to be supplemented by engineering judgment.

4.2. Effective Yield Moment (M_y)

Effective yield moment M_y (KN.m) for a steel coupling beam is given by Eqn. 4.1 based on multivariable regression analysis.

$$M_y = \alpha \cdot \left(\frac{d}{t_w}\right)^{-0.403} \cdot \left(\frac{b_f}{t_f}\right)^{-0.217} \cdot \left(\frac{L_c}{L_e}\right)^1 \cdot \left(\frac{L_c}{h}\right)^{-0.051} \cdot \left(\frac{h}{b_f}\right)^{2.764} \cdot (f_{yw})^{0.365} \cdot (f'_c)^{0.626} \quad (4.1)$$

In Eqn. 4.1 for steel coupling beam with stud bolts in embedment region $\alpha = 1.356$ and

For steel coupling beam without stud bolts in embedment region $\alpha = 1.043$

By checking the exponents of Eqn. 4.1 it is observed that the dependence of M_y on $\frac{h}{b_f}$ is much stronger than other parameters of equation. Values of M_y obtained from test results versus values of M_y obtained from Eqn. 4.1. is illustrated in Fig. 4.2.

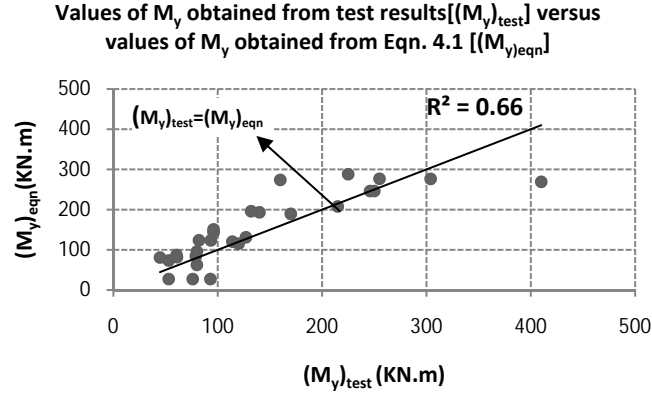


Figure 4.2. Values of M_y obtained from test results [$(M_y)_{test}$] versus values of M_y obtained from Eqn. 4.1 [$(M_y)_{eqn}$].

4.3. Capping Moment to Effective Yield Moment Ratio $\left(\frac{M_c}{M_y}\right)$

Capping moment to effective yield moment ratio $\frac{M_c}{M_y}$ for a steel coupling beam is given by Eqn. 4.2 based on multivariable regression analysis.

$$\frac{M_c}{M_y} = \left(\frac{d}{t_w}\right)^{-0.121} \cdot \left(\frac{b_f}{t_f}\right)^{-0.248} \cdot \left(\frac{L_c}{L_e}\right)^{0.032} \cdot \left(\frac{L_c}{h}\right)^{-0.084} \cdot \left(\frac{h}{b_f}\right)^{-0.09} \cdot (f_{yw})^{0.236} \cdot (f_c')^{0.002} \quad (4.2)$$

By checking the exponents of Eqn. 4.2 it is observed that the dependence of $\frac{M_c}{M_y}$ on $\frac{b_f}{t_f}$ and f_{yw} is much stronger than the other parameters of equation. Values of $\frac{M_c}{M_y}$ obtained from test results versus values of $\frac{M_c}{M_y}$ obtained from Eqn. 4.2 is illustrated in Fig. 4.3.

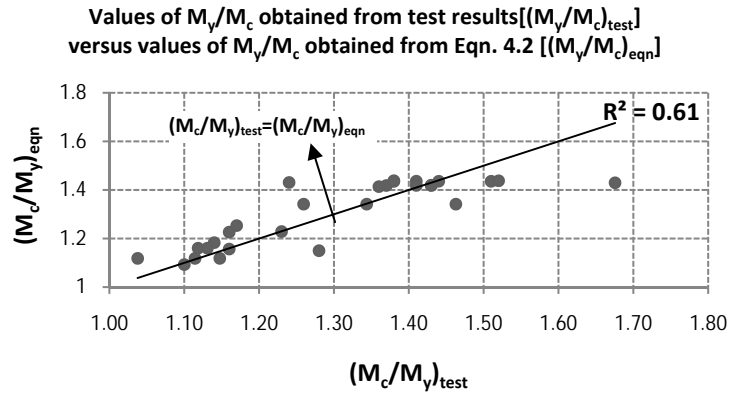


Figure 4.3. Values of M_y/M_c obtained from test results [$(M_y/M_c)_{test}$] versus values of M_y/M_c obtained from Eqn. 4.2 [$(M_y/M_c)_{eqn}$].

4.4. Cyclic Deterioration Parameters ($\Lambda_{s,c}$ and Λ_k)

The equation proposed to define the cyclic deterioration parameters for strength and post capping deterioration Λ_s and Λ_c respectively, is,

$$\Lambda_{s,c} = \beta \cdot \left(\frac{d}{t_w}\right)^{0.422} \cdot \left(\frac{b_f}{t_f}\right)^{0.175} \cdot \left(\frac{L_c}{L_e}\right)^{-1.576} \cdot \left(\frac{L_c}{h}\right)^{0.817} \cdot \left(\frac{h}{b_f}\right)^{-1.075} \cdot (f_{yw})^{-0.232} \cdot (f'_c)^{0.289} \quad (4.3)$$

In Eqn. 4.3 for steel coupling beam with stiffer or FBP or horizontal ties in embedment region $\beta = 1.123$ and

For steel coupling beam without stiffer and FBP and horizontal ties in embedment region $\beta = 0.194$

For unloading stiffness deterioration the proposed equation is,

$$\Lambda_k = \gamma \cdot \left(\frac{d}{t_w}\right)^{0.185} \cdot \left(\frac{b_f}{t_f}\right)^{-0.402} \cdot \left(\frac{L_c}{L_e}\right)^{-1.3} \cdot \left(\frac{L_c}{h}\right)^{1.169} \cdot \left(\frac{h}{b_f}\right)^{-0.647} \cdot (f_{yw})^{-0.23} \cdot (f'_c)^{0.885} \quad (4.4)$$

In Eqn. 4.4 for steel coupling beam with stiffer or FBP or reinforced concrete encasement $\gamma = 1.134$ and

For steel coupling beam without stiffer and FBP and reinforced concrete encasement $\gamma = 0.564$

Fig. 4.4. (a), (b) illustrates values of $\Lambda_{s,c}$ and Λ_k obtained from test results versus values of $\Lambda_{s,c}$ and Λ_k obtained from Eqn. 4.3 and 4.4 respectively.

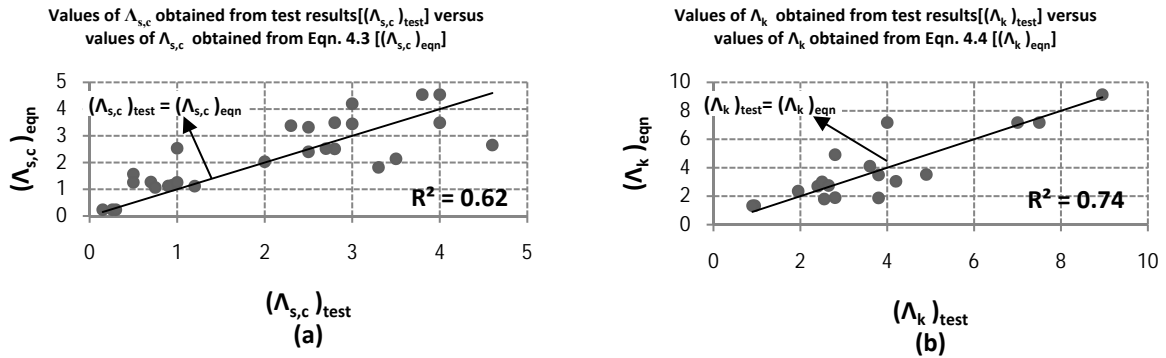


Figure 4.4. (a) Values of $\Lambda_{s,c}$ obtained from test results $[(\Lambda_{s,c})_{test}]$ versus values of $\Lambda_{s,c}$ obtained from Eqn. 4.3 $[(\Lambda_{s,c})_{eqn}]$, (b) Values of Λ_k obtained from test results $[(\Lambda_k)_{test}]$ versus values of Λ_k obtained from Eqn. 4.4 $[(\Lambda_k)_{eqn}]$

4.5. Plastic Rotation Capacity (θ_p)

Plastic rotation capacity θ_p (rad) for a steel coupling beam is given by Eqn. 4.5 based on multivariable regression analysis.

$$\theta_p = \eta \cdot \left(\frac{d}{t_w}\right)^{1.491} \cdot \left(\frac{b_f}{t_f}\right)^{-0.892} \cdot \left(\frac{L_c}{L_e}\right)^{-0.566} \cdot \left(\frac{L_c}{h}\right)^{-0.072} \cdot \left(\frac{h}{b_f}\right)^{-1.918} \cdot (f_{yw})^{-1.04} \cdot (f'_c)^{0.436} \quad (4.5)$$

In Eqn. 4.5 for steel coupling beam with FBP or reinforced concrete encasement $\eta = 1.139$ and

For steel coupling beam without FBP and reinforced concrete encasement $\eta = 0.858$

By checking the exponents of Eqn. 4.5 it is observed that the dependence of θ_p on $\frac{h}{b_f}$ is much stronger than other parameters of equation. Values of θ_p obtained from test results versus values of θ_p obtained from Eqn. 4.5 is illustrated in Fig. 4.5.

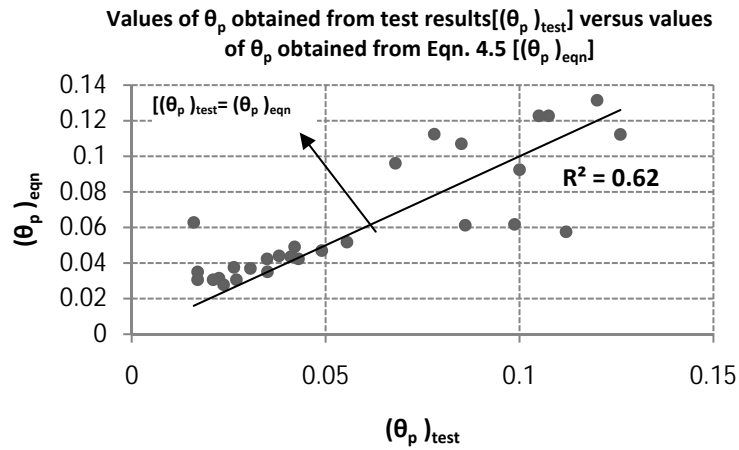


Figure 4.5. Values of θ_p obtained from test results $[(\theta_p)_{test}]$ versus values of θ_p obtained from Eqn. 4.5 $[(\theta_p)_{eqn}]$

4.6. Post Capping Plastic Rotation Capacity (θ_{pc})

Post capping plastic rotation capacity θ_{pc} (*rad*) for a steel coupling beam is given by Eqn. 4.6 based on multivariable regression analysis.

$$\theta_{pc} = \left(\frac{d}{t_w}\right)^{2.681} \cdot \left(\frac{b_f}{t_f}\right)^{0.11} \cdot \left(\frac{L_c}{L_e}\right)^{-2.447} \cdot \left(\frac{L_c}{h}\right)^{2.374} \cdot \left(\frac{h}{b_f}\right)^{-1.598} \cdot (f_{yw})^{-2.023} \cdot (f'_c)^{-0.03} \quad (4.6)$$

The values of θ_{pc} obtained from test results versus values of θ_{pc} obtained from Eqn. 4.6 is illustrated in Fig. 4.6.

For the development of predictive equations for θ_{pc} only specimens with clear indication of post-capping behavior are considered from tests.

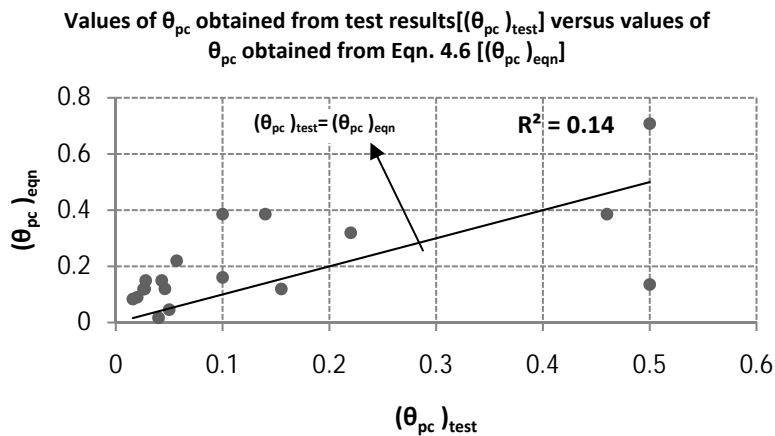


Figure 4.6. Values of θ_{pc} obtained from test results $[(\theta_{pc})_{test}]$ versus values of θ_{pc} obtained from Eqn. 4.6 $[(\theta_{pc})_{eqn}]$

4.7. Effective Stiffness (K_e)

The theoretically predicted elastic stiffness, K_e , of the steel coupling beams is determined using the

Eqn. 4.7 for cantilever beams:

$$K_e = \frac{3EI_{eq}}{L_{eff}^3} \quad (4.7)$$

Where I_{eq} is the equivalent second moment of area of the steel coupling beam accounting for the effect of shear deformation as determined from the following Eqn. 4.8.

$$I_{eq} = \frac{I_b}{1 + \frac{3EI_b}{L_{eff}^2 GA_w} \lambda} \quad (4.8)$$

Where I_b : second moment of area of the coupling beam (mm^4), E : Young's modulus for steel coupling beam (GPa), λ : cross-sectional shape factor for shear ($\frac{3}{2}$ for I-sections), G : shear modulus for steel coupling beam, A_w : web area of steel coupling beam excluding flanges (mm^2) and L_{eff} : effective length of beam (mm)

Modified equivalent second moment of area of the steel coupling beam accounting for the effect of the shear deformation, $(I_{eq})_m$ (mm), is given by the Eqn. 4.9 based on multivariable regression analysis.

Using $(I_{eq})_m$ instead of I_{eq} for determination of the elastic stiffness is recommended.

$$(I_{eq})_m = \frac{I_b(1 + \frac{3E\lambda}{L_{eff}^2 GA_w})}{1 + I_b(\frac{3E\lambda}{L_{eff}^2 GA_w})} \cdot \left(\frac{d}{t_w}\right)^{0.314} \cdot \left(\frac{b_f}{t_f}\right)^{0.206} \cdot \left(\frac{L_c}{L_e}\right)^{-1.182} \cdot \left(\frac{L_c}{h}\right)^{2.243} \cdot \left(\frac{h}{b_f}\right)^{0.168} \cdot (f_{yw})^{-0.503} \cdot (f_c)^{-0.396} \quad (4.9)$$

In Eqn. 4.9, $L_{eff} = \frac{L_c}{2} + \frac{L_e}{5}$ where L_c : clear span of beam (mm) and L_e : embedment length (mm).

5. CONCLUSIONS

The objective of the research discussed in this paper is to develop relationships for modeling component deterioration of steel coupling beams. The proposed relationships are empirical and are based on calibration of 28 moment- rotation diagrams of steel coupling beams from experimental tests.

The cyclic behavior of the steel coupling beam was evaluated using 28 specimens from the technical literatures. Multivariable regression analysis was used to evaluate the parameters controlling cyclic behaviour of these components. seven relationships were proposed to determine the effective yield moment M_y , capping moment to effective yield moment ratio $\frac{M_c}{M_y}$, plastic rotation capacity θ_p , post capping plastic rotation capacity θ_{pc} , effective stiffness K_e , cyclic deterioration parameter for strength and post capping deterioration $\Lambda_{s,c}$ and unloading stiffness deterioration parameter Λ_k .

These relationships can be used for modeling of deterioration parameters of plastic hinge regions in steel coupling beams.

REFERENCES

- Fortney, P. J. (2005). The next generation of coupling beams. *Dissertation, University of Cincinnati, Cincinnati*.
- Fortney, P. J., Shahrooz, B. M. and Rassati, G. A. (2007a). Large-scale testing of a replaceable "fuse" steel coupling beam. *Journal of Structural Engineering*. **133:12**, 1-7.
- Fortney, P. J., Shahrooz, B. M. and Rassati, G. A. (2007b). Seismic performance evaluation of coupled core walls with concrete and steel coupling beams. *Steel and Composite Structures*. **7:4**, 279-301.
- Gong, B. and Shahrooz, B. M. (2001a). Concrete-steel composite coupling beams. I: component testing. *Journal*

- of Structural Engineering*. **127:6**, 625-631.
- Gong, B. and Shahrooz, B. M. (2001b). Concrete-steel composite coupling beams. II: subassembly testing and design verification. *Journal of Structural Engineering*. **127:6**, 632-638.
- Harries, K. A. (1995). Seismic Design and Retrofit of Coupled Walls Using Structural Steel. *Dissertation, McGill University, Montreal*.
- Harries, K. A., Mitchell, D., Cook, W. D. and Redwood, R. G. (1993). Seismic Response of Steel Beams Coupling Concrete Walls. *Journal of Structural Engineering*. **119:12**, 3611-3629.
- Ibarra, L. F., Madina, R. A. and Krawinkler, H. (2005). Hysteretic models that incorporate strength and stiffness deterioration. *Earthquake Engineering and Structural Dynamics*, **34:12**, 1489-1511.
- Lignos, D. G., Krawinkler, H. and Whittaker, H. (2008). Shaking table collapse tests of a 4-story steel moment frame. *14th World Conference on Earthquake Engineering*, October 12-17, 2008, China.
- Lignos, D. G., Krawinkler, H. and Zareian, F. (2009). Modeling of component deterioration for collapse prediction of steel moment frames. *Stessa 2009, Taylor & Francis*, 403-409.
- Park, W. S. and Yun, H. D. (2005a). Seismic Behaviour of Steel Coupling Beam Linking Reinforced Concrete Shear Walls. *Engineering Structures*. **27**, 1024-1039.
- Park, W. S. and Yun, H. D. (2005b). Seismic Behaviour of Coupling Beams in a Hybrid Coupled Shear Walls. *Journal of Constructional Steel Research*. **61**, 1492-1524.
- Park, W. S. and Yun, H. D. (2006a). Seismic Behaviour and Design of Steel Coupling Beams in a Hybrid Coupled Shear Wall Systems. *Nuclear Engineering and Design*. **236**, 2474-2484.
- Park, W. S. and Yun, H. D. (2006b). The bearing strength of steel coupling beam-reinforced concrete shear wall connections. *Nuclear Engineering and Design*. **236**, 77-93.
- Park, W. S. and Yun, H. D. (2006c). Seismic performance of steel coupling beam- wall connections in panel shear failure. *Journal of Constructional Steel Research*. **62**, 1016-1025.
- Park, W. S. and Yun, H. D. (2006d). Panel shear strength of steel coupling beam- wall connections in a hybrid wall system. *Journal of Constructional Steel Research*. **62**, 1026-1038.
- Park, W. S., Yun, H. D., Hwang, S. K., Han, B. C. and Yang, I. S. (2005). Shear strength of the connection between a steel coupling beam and a reinforced concrete shear wall in a hybrid wall system. *Journal of Constructional Steel Research*, **61**, 912-941.
- Rahnama, M. and Krawinkler, H. (1993). Effects of soft soil and hysteresis model on seismic demands. *Report No. 108, John A. Blume Earthquake Engineering Center Stanford University, Stanford University*.
- Shahrooz, B. M., Remmetter, M. E. and Qin, F. (1993). Seismic Design and Performance of Composite Coupled walls. *Journal of Structural Engineering*. **119:11**, 3291-3309.